REVIEW

EDUCATIONAL SERIES IN CONGENITAL HEART DISEASE

Echocardiographic assessment of left to right shunts: atrial septal defect, ventricular septal defect, atrioventricular septal defect, patent arterial duct

Antigoni Deri MD and **Kate English MbChB PhD**

Yorkshire Heart Centre, Leeds Teaching Hospitals NHS Trust, Leeds, UK

Correspondence should be addressed to A Deri: a.deri@nhs.net

Abstract

This review article will guide the reader through the basics of echocardiographic assessment of congenital left to right shunts in both paediatric and adult age groups. After reading this article, the reader will understand the pathology and clinical presentation of atrial septal defects (ASDs), ventricular septal defects (VSDs), atrioventricular septal defects (AVSDs) and patent arterial duct. Echocardiography is the mainstay in diagnosis and follow-up assessment of patients with congenital heart disease. This article will therefore describe the echocardiographic appearances of each lesion, and point the reader towards specific features to look for echocardiographically.

Key Words

- atrial septal defect
- ventricular septal defect
- atrioventricular septal defect
- patent arterial duct
- echocardiography

Introduction

Congenital heart disease affects 8–12 infants per 1000 live births (1). In the United Kingdom, we perform around 10,000 surgical and interventional procedures for congenital heart defects every year. Congenital heart lesions are often detected antenatally or early in life, but diagnosis may be delayed until adulthood. Echocardiography is the perfect imaging tool for congenital heart defects; it is non-invasive, easily reproducible, relatively cheap and quick and gives excellent representation of the structural abnormalities faced. Other imaging modalities can provide complementary information, but transthoracic echocardiography is the workhorse of the congenital heart disease world, from initial diagnosis to long-term follow-up.

This review article aims to describe the echocardiographic features of left to right shunt lesions; atrial septal defect, ventricular septal defect, atrioventricular septal defect and patent arterial duct.

Clinical manifestations of left to right shunts

Shunt at the atrial level: A murmur at the pulmonary area, breathlessness and fatigue on exertion are the most common early symptoms, although usually not until later on in childhood. Rarely infants might present with congestive heart failure. It is not uncommon, though, for children to remain entirely asymptomatic until adulthood. Adults might complain of mild breathlessness or palpitations due to atrial arrhythmia as a result of right

atrial enlargement. ASDs can be an incidental finding due a systolic murmur, an abnormal chest X-ray or ECG while the patient is being assessed for other problems.

Shunt at the ventricular level or the duct: These present early on in life with increased work of breathing, difficulty with feeding and poor weight gain. A murmur might not be audible immediately after birth due to the elevated pulmonary vascular resistance. As this falls in the subsequent weeks, a large defect will cause increased pulmonary blood flow leading to congestive heart failure, and the infant will be more susceptible to respiratory infections. Small ventricular defects can be detected incidentally due to a heart murmur. They are usually managed conservatively but patients might present with secondary problems such as endocarditis, aortic regurgitation, subaortic obstruction and double-chambered right ventricle.

Large ducts in preterm babies that do not respond to medical therapy will in some cases render the infant ventilator dependent until the duct is closed. Small ducts may present with endocarditis, incidental murmur or abnormal calcification on the chest X-ray.

Patients with sizeable left to right shunt that have been left untreated may develop pulmonary vascular disease and progressive increase in the pulmonary vascular resistance. When the latter exceeds the systemic vascular resistance the direction of shunt reverses and becomes right to left, a condition known as Eisenmenger's syndrome.

Common haemodynamic features in shunt lesions

Left to right shunts share common haemodynamic features, which should be assessed by 2D imaging, colour flow Doppler mapping and spectral Doppler. We will review them before discussing each lesion individually:

- Size of the shunt: The size of the shunt is proportional to the size of the defect and the relative resistances of the systemic and pulmonary vascular beds.
- Direction of flow: This is usually left to right. The flow across the ASD is phasic occurring predominantly in late ventricular systole and early diastole with augmentation of the shunt during atrial contraction (2). The shunt across the VSD is present throughout the cardiac cycle and provides increased blood flow to the pulmonary circulation, resulting in left heart dilatation. Right to left or bidirectional shunt can be seen in the setting of significant pulmonary hypertension or impaired right ventricular (RV) compliance.
- Chamber dilatation: Left to right shunts lead to volume overload of the cardiac chambers; atrial shunts cause dilatation of the right atrium (RA) and RV. Shunts at the ventricular level and ducts cause left heart dilatation.

Guidelines have been published regarding the RV morphometric evaluation for children (3) and adults (4). In children, this can be challenging with two-dimensional (2D) echocardiography as measurements are underestimated when compared with MRI in children (5) as opposed to adults (6). 3D echocardiography (3DE) offers more reproducible and comparable measurements (7, 8, 9). In children, the LV dimensions should be indexed to body surface area.

- Elevated pulmonary arterial pressure: Large left to right shunts result in elevated pulmonary arterial pressure and resistance. The systolic RV pressure can be estimated by the peak velocity of the tricuspid regurgitation (TR) or by continuous-wave Doppler interrogation of the flow across the VSD (Fig. 1). Diastolic pulmonary pressure can be calculated from the peak and end-diastolic velocities of pulmonary regurgitation, if present.
- The shape of the interventricular septum (IVS): In RV volume overload, the IVS is displaced towards the LV in diastole with subsequent septal flattening. Presence of pulmonary hypertension will lead to systolic septal flattening.
- Qp:Qs: The left to right shunt can be expressed as pulmonary (Qp) to systemic (Qs) blood flow ratio and calculated using the continuity equation (10):

$$Qp/Qs = RVOT\ VTI \times RVOT\ area / LVOT\ VTI \times LVOT\ area$$

RVOT = right ventricular outflow tract, LVOT = left ventricular outflow tract, VTI = velocity time integral.

Paradoxically, in patients with a persistent duct, the area of the RVOT and corresponding VTI are used to calculate the systemic blood flow and the pulmonary blood flow is calculated using the LVOT area and VTI. Qp: Qs should be used cautiously as there are potentially sources of error. The calculation of the RVOT and LVOT area is based on the measurement of the diameter of these outflow tracts, which is then squared in order to calculate the corresponding area. This renders the estimation of Qp:Qs highly sensitive to errors as small differences in the measurement will lead to significant discrepancies in the final result. Moreover, the measurement of the RVOT

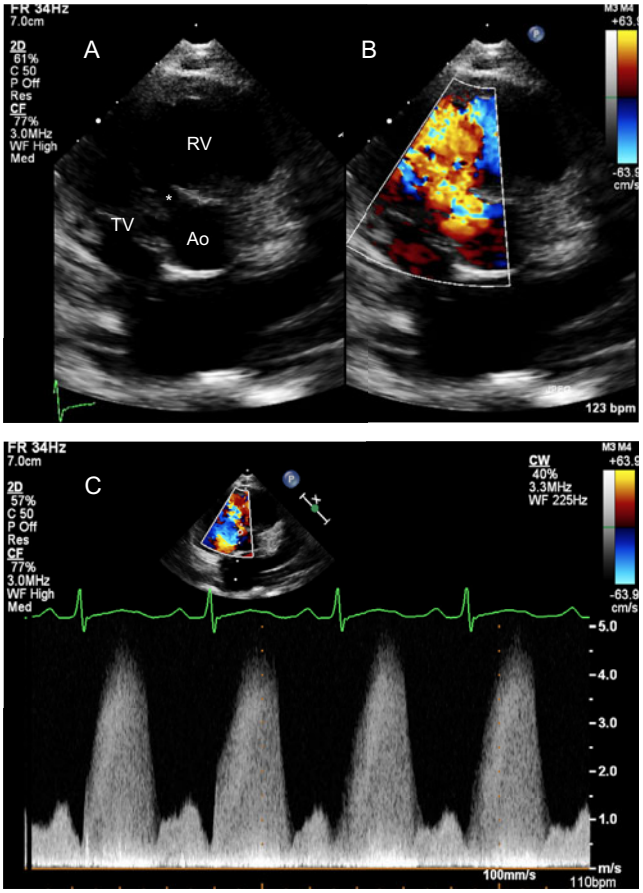

Figure 1
Parasternal short-axis view showing a perimembranous VSD (*) partially covered by aneurysmal tricuspid valve tissue in 2D (A) and colour Doppler (B). (C) Shows the Continuous Doppler trace across the defect. The Bernoulli equation allows the calculation of the pressure gradient (PG) between the right and left ventricles, in this case PG = 4 × 4.72 = 88.36 mmHg. The left vent ricular systolic pressure is assumed to be equal to the cuff-measured systolic pressure provided, there is no left ventricular outflow tract obstruction. In this case, the systolic blood pressure of the patient was 115 mmHg. The right ventricular pressure will be the difference of the LV systolic pressure and the PG between the two ventricles = 115–88.36 = 26.64 mmHg.

can be challenging given the sometimes challenging or inadequate windows. Cardiac catheterisation and cardiac MRI allow a quantitative approach in the calculation of pulmonary to systemic flows.

- Ventricular function: RV function can be affected particularly in the context of pulmonary hypertension. Older patients with significant atrial shunt can have LV diastolic dysfunction that becomes unmasked following closure of the ASD (11).
- Effect on outflow tracts: A large shunt can exaggerate the pressure gradient across the outflow tracts e.g. a large atrial shunt can increase the pressure gradient across the pulmonary outflow tract.
- Secondary effects: For example, a significant VSD might lead to dilatation of the mitral valve annulus and subsequent mitral regurgitation.
- Association with other congenital cardiac malformations: The echocardiographic investigation should be thorough, following a sequential segmental approach. Some of those malformations might be unmasked only after the shunt lesion is closed e.g. the severity of a mitral stenosis may become apparent after closure of a large ASD.

Atrial septal defects (ASDs)

Types of interatrial communications

The *ostium primum defect* is a type of atrioventricular septal defect characterised by the presence of a common atrioventricular (AV) junction without a ventricular component to the defect. This will be described in the AVSD section (Fig. 2).

Ostium secundum defects are true deficiencies in the primary septum and the most common type of interatrial communication. They vary in shape and size and can be single or multiple.

Sinus venosus defects are not true ASDs. These are venous abnormalities characterised by the anomalous insertion of right pulmonary veins into the wall of the superior vena cava (SVC). The SVC enters the atrial mass so that it 'over-rides' the atrial septum permitting flow

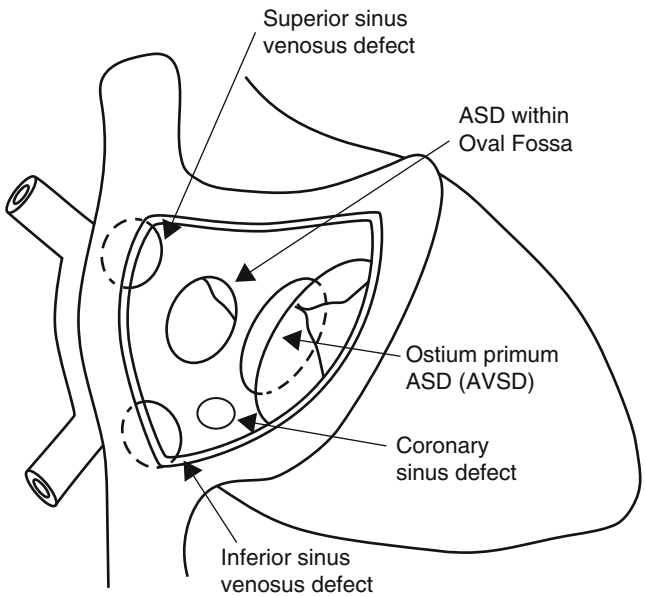

Figure 2
Different types of interatrial communications.

www.echorespract.com
https://doi.org/10.1530/ERP-17-0062

from the left atrium to the right atrium. A sinus venosus defect at the orifice of the inferior vena cava will create an inferior interatrial communication.

Coronary sinus (CS) defects are a type of communication between the atriums through the mouth of the sinus. The deficiency between the adjacent walls of the CS and the left atrium (LA) may vary from small fenestrations to complete absence resulting in partial or complete unroofing of the CS. The latter is associated with dilatation of the CS ostium due to the large left to right shunt and drainage of a persistent left SVC to the LA roof (12).

Rarely all components of the atrial septum are absent resulting in a *common atrium* (13).

Echocardiographic assessment

The atrial septum should be assessed from subcostal, apical and parasternal views:

Subcostal

The preferred acoustic window. The atrial septum is seen in the anterior-posterior (four-chamber view, Fig. 3) and superior-inferior axis (sagittal view). The latter allows assessment of the margins to the SVC and IVC and is the optimal window for imaging a sinus venosus defect (Fig. 4). The left anterior oblique (LAO) view shows the length of the atrial septum and demonstrates the ostium primum defect (Fig. 5) as well as dilatation of the CS if present. Partially or completely unroofed CS can be seen from this view. Colour Doppler interrogation and contrast studies can be performed.

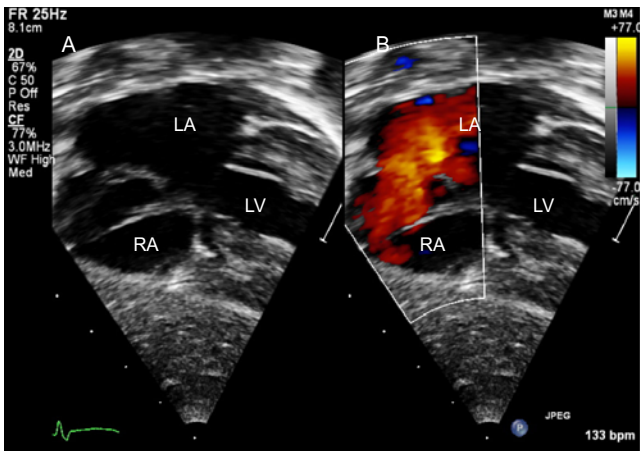

Figure 3
Subcostal four-chamber view shows a large ostium secundum ASD on 2D (A) and colour Doppler (B).

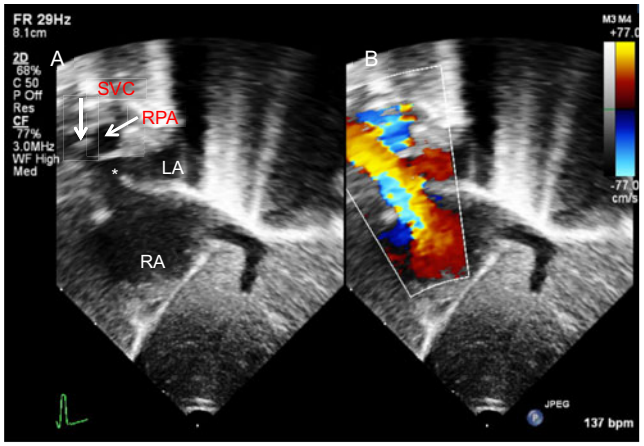

Figure 4
Superior sinus venosus defect (*) demonstrated from subcostal sagittal view on 2D (A) and Colour Doppler (B).

Apical four chamber

In this view, the ultrasound beam is parallel to the atrial septum and measurements should be avoided, as there is risk of an artificial dropout. The four-chamber view allows haemodynamic assessment of the ASD (RA and RV dilation, Fig. 6) and estimation of the RV pressure based on the TR jet velocity.

Parasternal short axis (PSAX)

The atrial septum is seen posterior to the aortic root and thus the aortic rim of the defect can be identified (Fig. 7). Sinus venosus and postero-inferior defects can also be seen in this view but measurements of the defect are not recommended due to the risk of drop out.

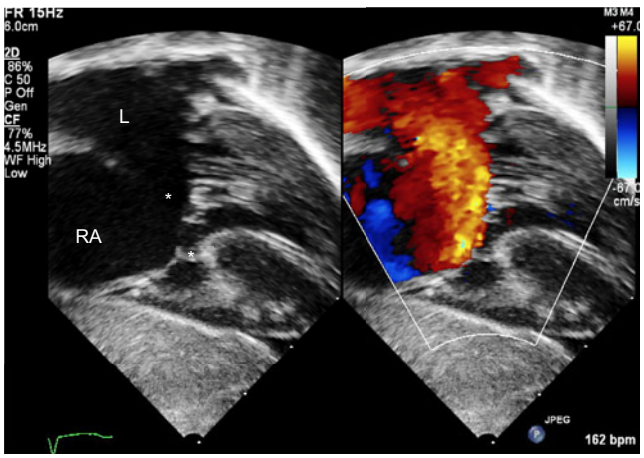

Figure 5
Subcostal view showing a primum atrial septal defect (*). The bridging leaflets of the common valve are attached to the crest of the septum (**) allowing shunt only at the atrial level. This is a partial AVSD.

www.echorespract.com
https://doi.org/10.1530/ERP-17-0062

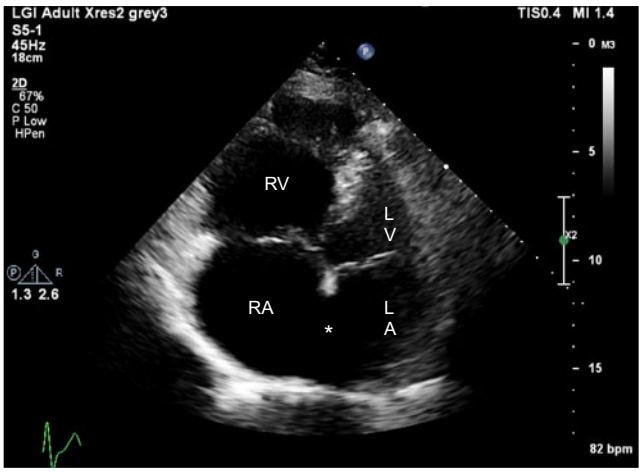

Figure 6
Dilated right atrium and right ventricle in an adult with a large secundum ASD (*).

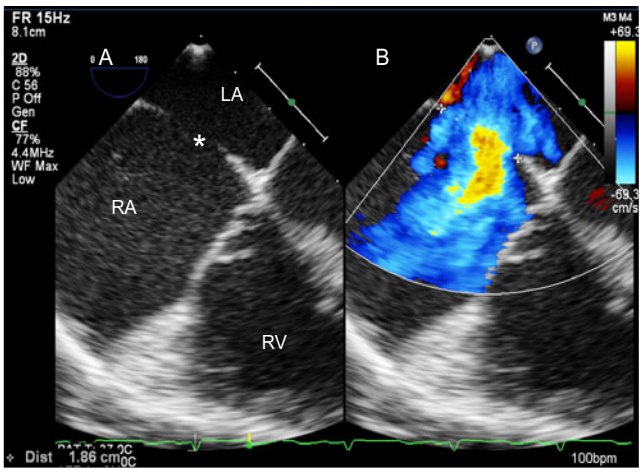

Figure 8
Four-chamber TOE view (mid-oesophageal, 0°) on 2D (A) and colour Doppler (B). The maximum dimension of the ASD is measured and its relationship with the AV valves assessed.

High right parasternal

The patient is positioned in the right lateral decubitus position with the probe in a superior-inferior orientation. This view is ideal for detection of sinus venosus defects.

In young children TTE will usually allow a full diagnostic study. In older children and adults, in particular, those considered for a transcatheter device closure, transoesophageal echocardiography (TOE) offers additional valuable information (Figs 8, 9, 10, 11 and 12). Table 1 summarises the basic TOE views for the assessment of ASDs. As with TTE, the location, size and number of defects should be identified as well as the relationship with the surrounding structures, in particular in patients considered for a percutaneous device closure. The American Society of Echocardiography has published comprehensive guidelines for the TOE examination (14) and for the assessment and percutaneous closure of ASDs with transthoracic, transoesophageal and intracardiac echocardiography (15).

In patients with poor acoustic windows, contrast echocardiography is another alternative in selected patients (15). Intravenous injection of agitated saline in the left arm is very useful in the investigation of a left SVC in the context of a completely unroofed CS; imaging from the apical four-chamber view will reveal the presence of contrast in the left upper corner of the LA and subsequently in the RA.

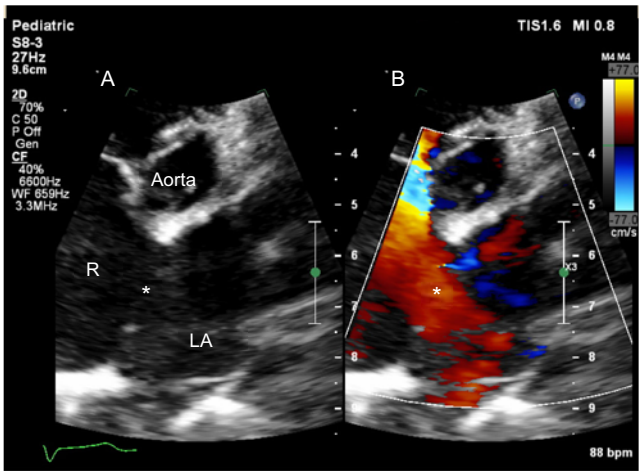

Figure 7
Parasternal short-axis view on 2D (A) and colour Doppler (B) showing a large secundum ASD (*). Note the dilated right atrium (RA).

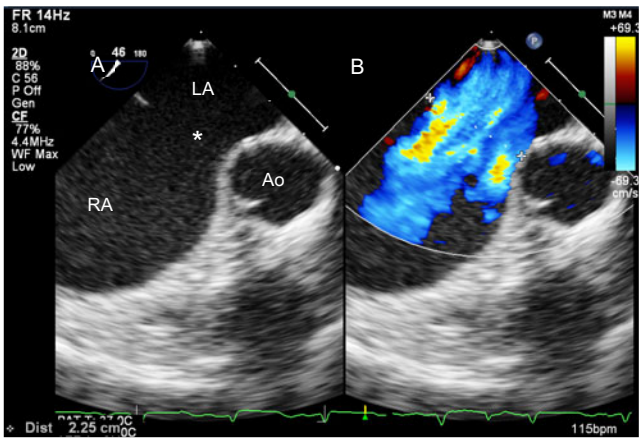

Figure 9
Transoesophageal view (mid-oesophageal, approximately 45°) of a large ASD on 2D (A) and colour Doppler (B). The aortic rim is deficient.

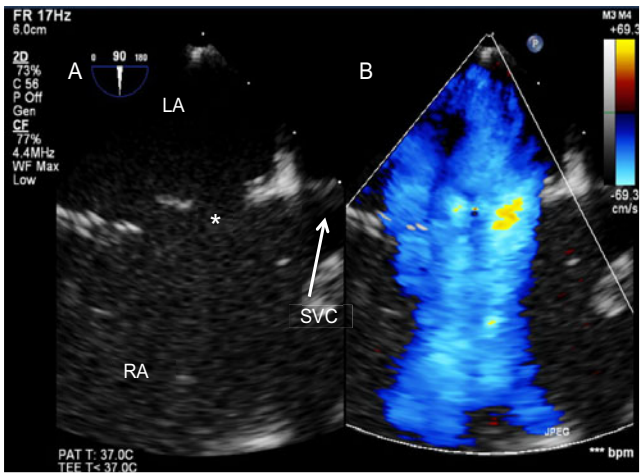

Figure 10
Large atrial shunt secondary to multiple defects seen from the bicaval TOE view (mid-oesophageal, 90°) on 2D (A) and colour Doppler (B).

Management and follow-up of ASDs

Large ASDs or those associated with paradoxical embolism or platypnoea/orthodeoxia should be closed. Irreversible pulmonary hypertension is the only absolute contraindication for closure. Secundum type defects with adequate rims can be closed percutaneously (Fig. 13). Following device closure, the position of the device, the relationship to surrounding structures, any residual shunts should be carefully evaluated. Follow-up continues lifelong every 1–2 years due to risk of erosion (16). Patients post-surgical closure with no other cardiac abnormalities are usually discharged after a year although a small but definite incidence of atrial arrhythmias has been described even years after the repair (17, 18).

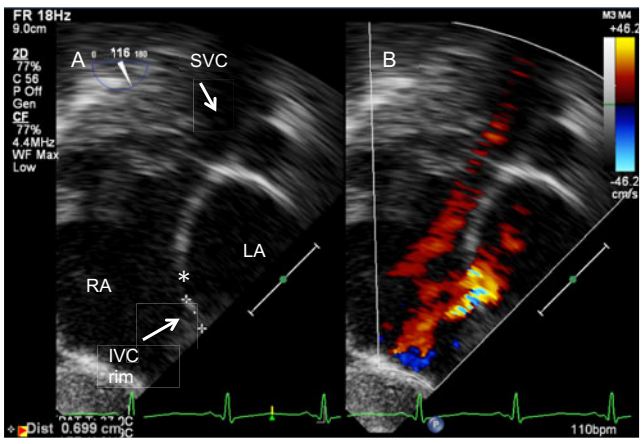

Figure 11
Assessment of ASD (*) for device closure. The IVC rim is seen from the transgastric bicaval view (116°) on 2D (A) and colour Doppler (B).

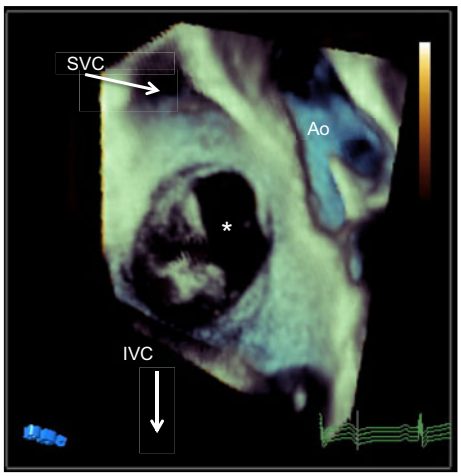

Figure 12
TOE 3D view of the atrial septum from the RA side. The ASD is noted with *.

Ventricular septal defects (VSDs)

Epidemiology and morphology

Ventricular septal defects are the most common congenital heart lesion, occurring in approximately 33% of patients with congenital heart disease (19). They may occur in isolation or as part of more complex congenital heart disease. Depending on their right ventricular borders they can fall into one of three categories:

Perimembranous defects

Perimembranous defects are located in the membranous septum. When viewed from the right ventricle, these lesions are located towards the inner curvature of the heart. Their location leads to continuity between the tricuspid and aortic valves. This type may extend into the inlet or outlet part of the right ventricle or may be large enough to shunt towards all RV components.

Perimembranous defects may close due to the proximity of the septal leaflet of the tricuspid valve to these defects; aneurysmal tissue from the underside of the leaflet might partially or completely cover the hole.

Alternatively, the right coronary cusp and sometimes the non-coronary cusp may prolapse through the defect with subsequent reduction of the size of the defect or even complete occlusion, often at the expense of aortic regurgitation.

Muscular defects

Muscular defects have completely muscular borders, they can be single or multiple and located anywhere within the septum.

www.echorespract.com
https://doi.org/10.1530/ERP-17-0062

Table 1 Transoesophageal views for the assessment of ASD.

View	Position in the oesophagus	Multiplane angles	Anatomical features
Four chamber	Mid-oesophagus	0°, 15°, 30°	Relationship to the AV valves Posterior rims ASD diameter
Upper oesophageal short axis	Mid- to upper oesophagus	0°, 15°, 30°, 45°	SVC rim Right upper pulmonary vein Superior aortic rim Detection of sinus venosus defect
Mid-oesophageal aortic valve short axis	Mid-oesophagus	30°, 45°, 60°, 75°	Posterior and aortic rims PFO ASD diameter
Bicaval view	Mid-oesophagus	90°, 105°, 120°	IVC and SVC rims Anomalous pulmonary venous drainage ASD diameter
Long axis	Mid- to upper oesophagus	120°, 135°, 150°	Roof of the LA Left pulmonary veins

AV, atrioventricular; IVC, inferior vena cava; LA, left atrium; SVC, superior vena cava.

Juxtaarterial and doubly committed defects

Juxtaarterial and doubly committed defects are characterised by fibrous continuity between the adjacent leaflets of the aortic and pulmonary valves. The outlet septum and septal component of the subpulmonary infundibulum are absent. The aortic sinus may prolapse into the defect resulting in partial or complete closure at the cost of aortic regurgitation (20).

This classification of VSDs follows the European approach and focuses on the anatomic features immediately adjacent to the defect, the so-called *border approach*. An alternative approach is *geographical*, which focuses primarily on the position of the hole within the ventricular septum and classifies VSDs as central, inlet, outlet and muscular. Understandably, there is an on-going debate and effort to achieve an international consensus for VSD definition and categorisation (21, 22).

Echocardiographic assessment

Multiple windows, planes and sweeps should be used to assess the ventricular septum.

The perimembranous VSD can be demonstrated on the PSAX (Fig. 14) and apical four-chamber views (Fig. 15). Its relationship to the aortic valve can be seen from apical long axis and PLAX views. Occasionally, these defects are covered by apposition of the septal leaflet of the tricuspid valve and may close spontaneously, either partially or completely. Associated findings such as double-chambered

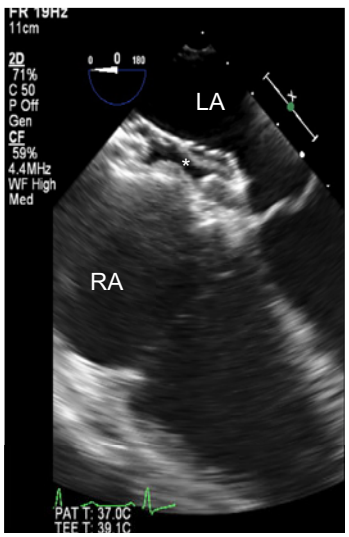

Figure 13
TOE mid-oesophageal view at 0° showing an ASD device *in situ* following percutaneous ASD closure.

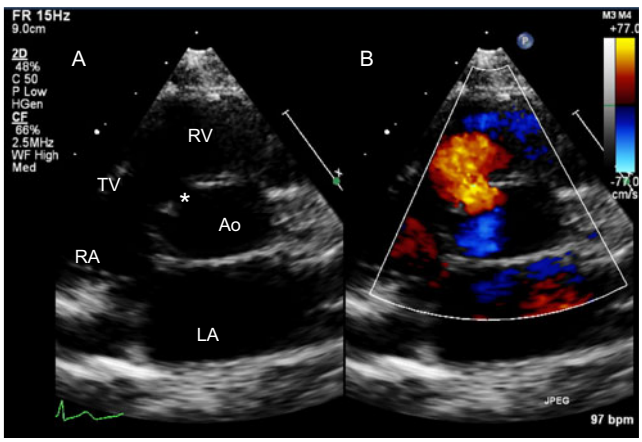

Figure 14
A perimembranous VSD is shown in the PSAX TTE view in 2D (A) and colour Doppler (B). Note the tricuspid-aortic valve fibrous continuity.

www.echorespract.com
https://doi.org/10.1530/ERP-17-0062

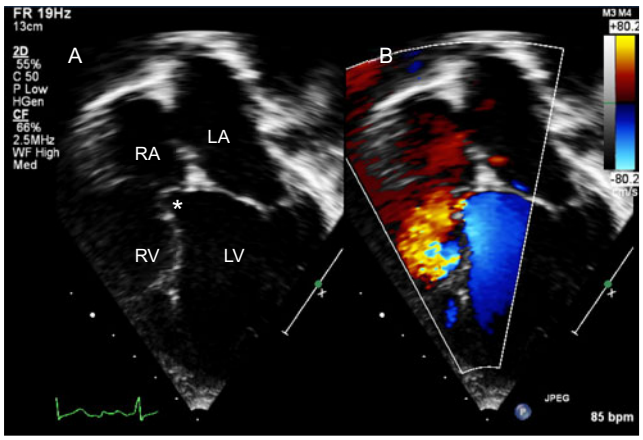

Figure 15
Perimembranous VSD partially covered by tricuspid valve tissue.

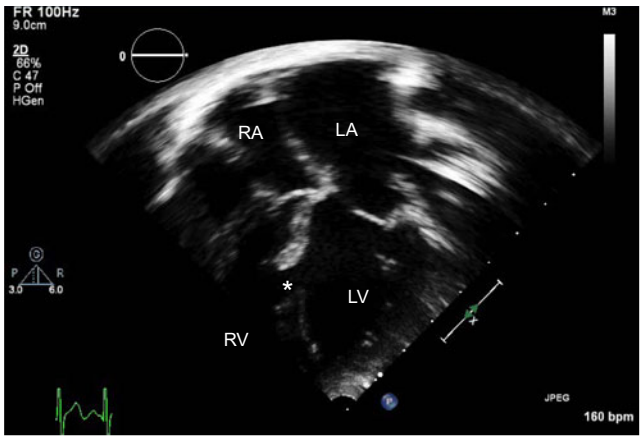

Figure 16
Large muscular VSD (*). The LA and LV are significantly dilated.

RV, a Gerbode defect or subaortic ridge can be seen with perimembranous VSDs. The right or non-coronary cusp of the aortic valve can prolapse into the defect leading to a new onset aortic regurgitation.

Muscular VSDs (Fig. 16) are located at either the inlet, outlet or trabecular portion of the septum and can be singular or multiple. The septum should be interrogated thoroughly at its entire length by sweeping from subcostal, apical and parasternal views (Video 1). Colour flow Doppler can identify small VSDs that are not visible on 2D. The sensitivity of this is reduced in newborns with persistent fetal circulation or patients of any age with elevated RV pressure.

Video 1

Multiple VSDs sweep. View Video 1 at http://movie-usa.glencoesoftware.com/video/10.1530/ERP-17-0062/video-1.

Doubly committed and juxtaarterial VSDs are best seen from the PSAX view (Fig. 17, Video 2) as well as the PLAX with slight counter clockwise rotation of the transducer. The unsupported right coronary cusp of the aortic valve can potentially prolapse into the defect leading to distortion of the leaflet and variable degree of aortic insufficiency (Video 3).

Video 2

DCVSD short axis. View Video 2 at http://movie-usa.glencoesoftware.com/video/10.1530/ERP-17-0062/video-2.

Video 3

DCVSD Ao prolapse View Video 3 at http://movie-usa.glencoesoftware.com/video/10.1530/ERP-17-0062/video-3.

Location of defect(s)

The PSAX view is very useful in identifying the location of the VSD(s). A cut at the level of the aortic valve will show a perimembranous VSD between 9 o'clock and 11 o'clock positions (Fig. 14). Occasionally, these defects are partially covered by tricuspid valve aneurysmal tissue and their size can be underestimated on 2D, but colour flow Doppler will reveal the magnitude of flow. Anterior extension of these defects will be seen between 11 and 12 o'clock. Doubly committed defects are identified between 12 and 2 o'clock (pulmonary valve hinge point) (Fig. 17). A sweep performed from the PSAX view beginning from the aortic valve towards the apex can profile muscular VSDs. Anterior muscular VSDs will be seen between

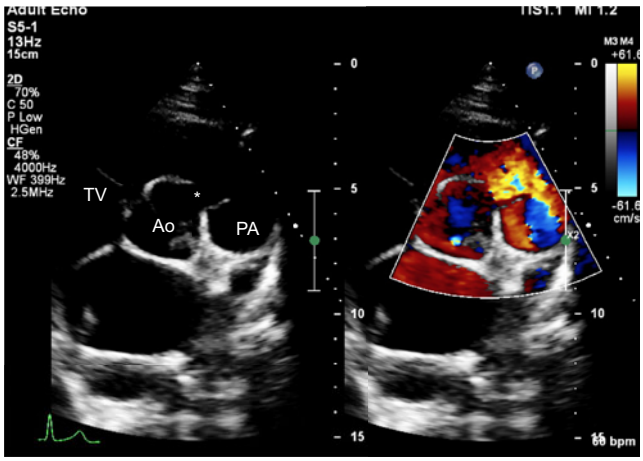

Figure 17
Parasternal short-axis view showing a doubly committed VSD (*). The right coronary cusp of the aortic valve has a mildly elongated appearance as it is prolapsing through the defect, partially covering it. The aortic and pulmonary valves are in fibrous continuity.

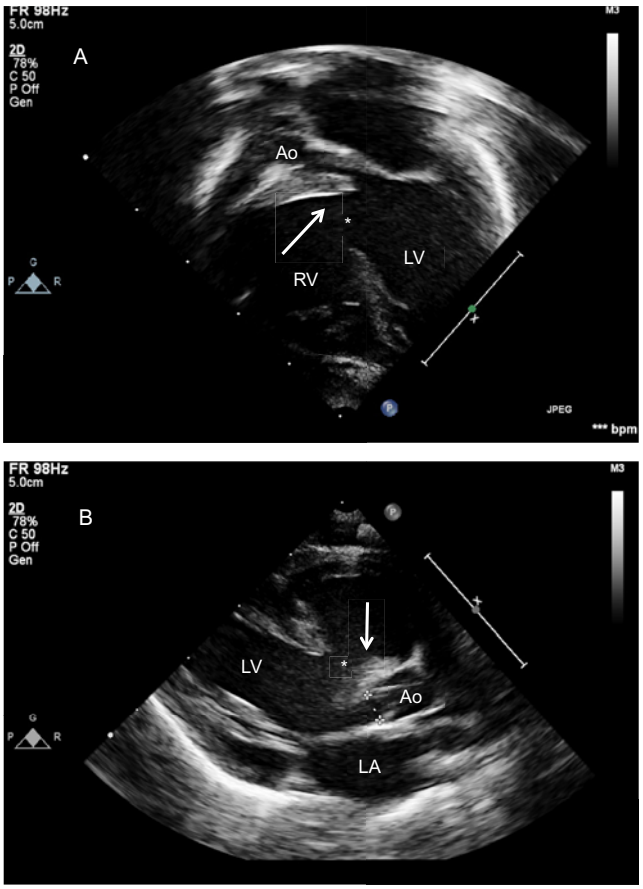

Figure 18
Large malalignment VSD (*) as seen from the apical four-chamber view with anterior angulation to open the left ventricular outflow tract (A) and parasternal long axis view (B). The outlet septum is posteriorly deviated (arrow) creating a very narrow outflow tract. This newborn also had a small, bicuspid aortic valve and interruption of the aortic arch.

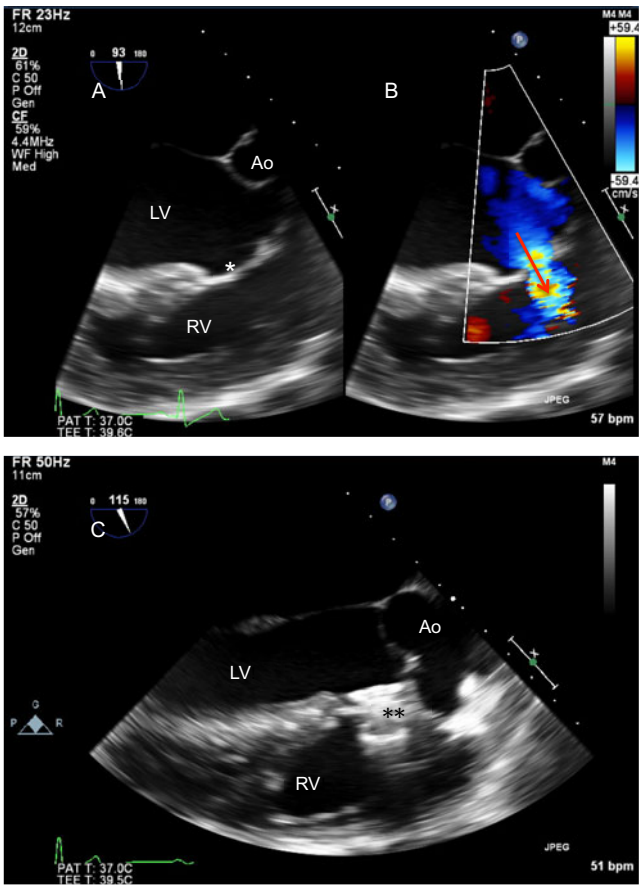

Figure 19
TOE in a patient with previous surgical closure of a large VSD (* in image A is in the position of the patch) with a fenestration allowing a residual shunt as shown with colour Doppler (arrow in image B). (C) Post percutaneous device closure of the defect (**).

12 and 2 o'clock, mid-muscular between 10 and 12 o'clock and posterior muscular between 7 and 10 o'clock (23).

The echocardiographer should look for malalignment of the outlet septum (Fig. 18), straddling AV valves, aortic cusp prolapse and other associated abnormalities and also measure the defect margins for consideration of transcatheter closure.

Newborns and young children usually have excellent acoustic windows that will allow a thorough transthoracic echocardiographic assessment. In those patients in whom TTE imaging is limited the TOE is an excellent alternative particularly when there are haemodynamically associated lesions or the defect is considered for percutaneous closure (Fig. 19).

Management

Asymptomatic infants with a restrictive VSD and no evidence of pulmonary hypertension will not require treatment. Indication for closure in these patients will be the development of complications (aortic cusp prolapse, subaortic ridge, double-chambered RV, endocarditis). Infants with a significant shunt will develop congestive heart failure and will be referred for surgery. Percutaneous device closure is an alternative for a small and carefully selected population, usually older children with muscular or perimembranous defects with sufficient rims.

Atrioventricular septal defects (AVSDs)

Epidemiology and morphology

Atrioventricular septal defects make up 4–5% of all congenital heart defects, occurring in 34.8 per 100,000 live births (24). There is a very strong association between AVSD and Down's syndrome. Bergström and coworkers described up to 42% of patients with Trisomy 21 and congenital heart disease having an AVSD (25).

The cardinal feature of all AVSDs is the presence of a common AV junction rather than separate right and left AV junctions. This common junction is guarded by a distinctive AV valve (Fig. 20), which in the majority of cases has a common AV orifice and consists of five leaflets. Occasionally, the common valve may be divided into two orifices (right and left) under the conditions of dense attachments to the ventricular septum, dense attachments to the atrial septum (AVSD with no primum defect) or divided by a tongue of tissue. Regardless of common or separate orifices, the left component of the common AV valve has three leaflets that have no counterparts in the mitral valve of the normal heart. The left mural leaflet is exclusively in the LV. The other two are the bridging leaflets and are attached to variable extent with tension apparatus into both ventricles. The left ventricular component of the bridging leaflets serves as a commissure and is often described incorrectly as a 'cleft'.

AVSDs can be classified depending on the level of shunting across the defect. It is this anatomical feature that influences the clinical presentation.

- When neither of the bridging leaflets is attached to the septal components, there is obligatory shunt at both atrial and ventricular levels. The degree of ventricular shunt will depend on the proximity of the bridging leaflets to the crest of the ventricular septum.
- When leaflets are attached to the ventricular crest, the shunt will be at the atrial level. These are the so-called *partial AVSDs* or *ostium primum defects* and have no ventricular component. In partial AVSDs, the common valve has two orifices.
- When leaflets are fused to the underside of the atrial septum, the shunt will be at the ventricular level.

The AVSDs may be either balanced or unbalanced at the ventricular level. In the latter, the common AV valve opens predominantly to one ventricle, and there is associated hypoplasia of the contralateral ventricle. Unbalance might also be noted at the atrial level; malaligned atrial septum as well as double outlet atrium have been described (26).

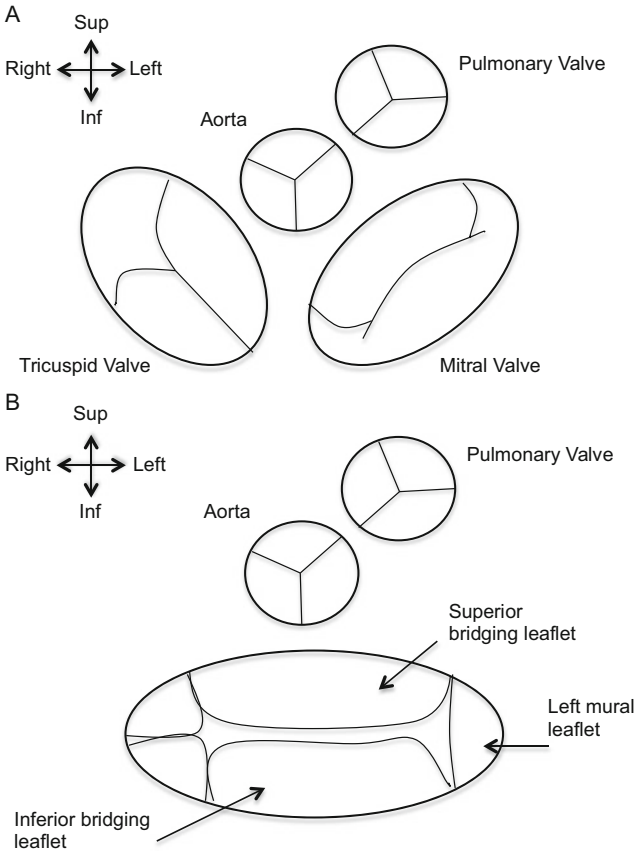

Figure 20
(A) Normal arrangement of atrioventricular and semilunar valves. In the normal heart the aortic and mitral valves are in fibrous continuity. (B) Common AV valve instead of normal Tricuspid and Mitral valves in AVSD. Note the 'unwedged' position of the Aorta in the AVSD setting. The Aorta maintains its fibrous continuity with the common AV valve.

Echocardiographic assessment

TTE provides excellent visualisation of the anatomy of AVSD and along with colour and spectral Doppler allows a comprehensive evaluation of the defect.

Subcostal views

The long axis and LAO view demonstrate the primum defect as well as any additional atrial communications (Fig. 5). The subcostal short axis and LAO views show the abnormal elongation of the left ventricular outflow tract due to unwedging of the aortic outflow gives the appearance of 'goose-neck deformity' (Fig. 21). The subcostal LAO allows the view of the common AV valve en face and can be used to determine the balance of the valve over the ventricles (Video 4). The subcostal short-axis view shows the anatomy of the AV valves and helps differentiate them from normal mitral and tricuspid valves. The size of the mural leaflet and the papillary muscles of the left AV valve can be identified in this view. A small mural leaflet and single papillary muscle have been associated with imbalance of the left AV valve and worse prognosis (27).

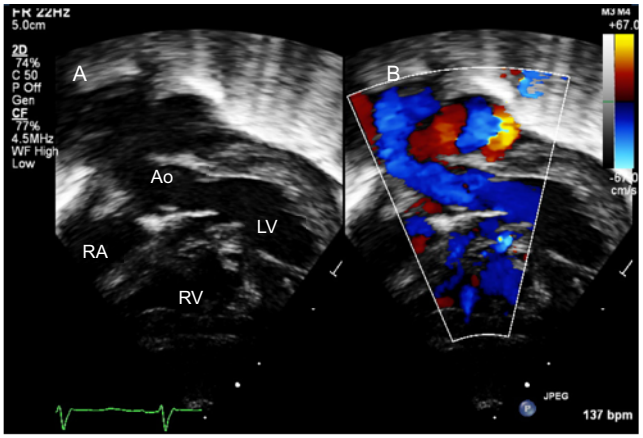

Figure 21
Subcostal left anterior oblique view of an infant with AVSD showing the 'goose-neck deformity' of the left ventricular outflow tract.

Video 4

En face view of AV valve. View Video 4 at http://movie-usa.glencoesoftware.com/video/10.1530/ERP-17-0062/video-4.

Apical view

Both AV valves as well as the relationship of the common AV valve within the defect are seen in this view (Fig. 22). Posterior to anterior sweep will reveal the VSD and can demonstrate chordal attachments to the ventricular septum. Colour Doppler will show the AV valve inflow and regurgitation. The LVOT can be assessed from the apical 5-chamber view. Obstruction of the LVOT can be seen either before or after surgical repair and could be due to chordal attachments to the LV side of the septum, subaortic membrane, septal hypertrophy, anomalous or prominent papillary muscle.

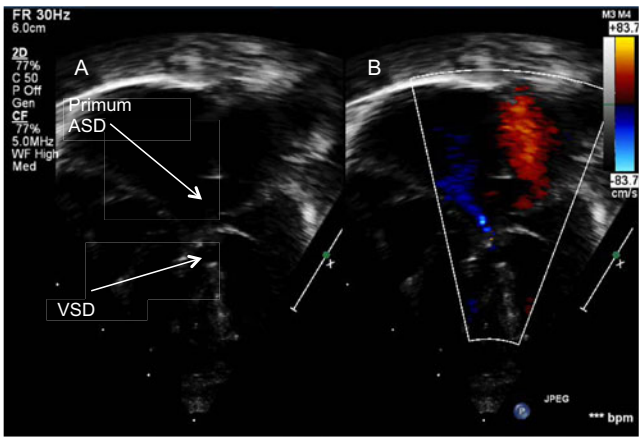

Figure 22
AVSD with large atrial and ventricular components seen from the apical four-chamber view on 2D (A). Colour Doppler (B) shows a mild degree of central AV valve regurgitation.

PLAX view

The AV valve regurgitation is further assessed from this view. Abnormal chordal attachments or a subaortic membrane may be identified (Fig. 23).

PSAX view

This will demonstrate the VSD and identify additional ventricular defects. The AV valves can be seen in the short axis and the origin of regurgitation was assessed.

AVSDs may be associated with other congenital defects such as Tetralogy of Fallot, isomerism of the atrial appendages, anomalous pulmonary venous drainage

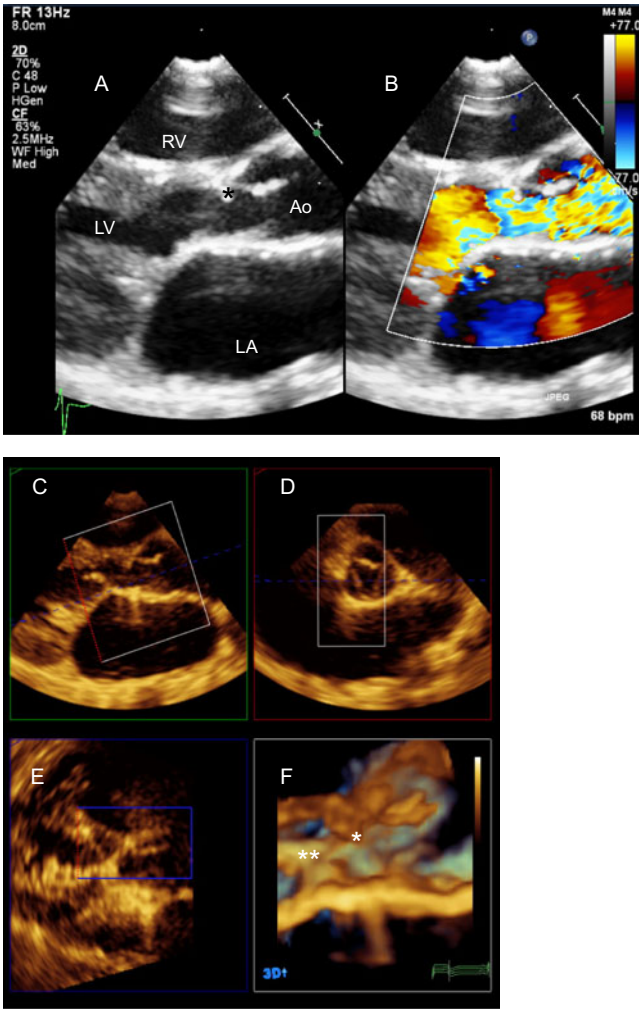

Figure 23
Patient several years post repair of AVSD with significant subaortic obstruction. (A) PLAX reveals a subaortic membrane (*) but colour Doppler (B) demonstrates presence of turbulence below the level of the membrane. A 3D volume was acquired from the PLAX window. MPR showed chordal attachments to the LVOT (**) in addition to the subaortic membrane (*) (C and F). The excursion of the aortic leaflets is limited secondary to the membrane (D).

and the echocardiographer should perform a careful assessment in the usual sequential segmental approach.

Unbalanced AVSD

Unbalance of the atria should be assessed from the apical four-chamber view. The atrial and AV valve inflows are evaluated by colour, pulse-wave and continuous-wave Doppler to look for presence of obstruction and assess its severity.

Ventricular imbalance is assessed from several views and various techniques have been proposed: En face view of the AV valve from the subcostal LAO allows the calculation of the modified AV valve index (AVVI = Left AV valve area: Total AV valve area) (28) (Fig. 24). AVVI between 0.4 and 0.6 is suggestive of balanced AVSD. Other parameters such as RV:LV inflow angle, the LA overriding the left AV valve, size parameters of the LV inflow (29), the direction of flow at the VSD in systole and in the transverse arch as well as the presence of any obstruction are felt to be likely surrogates of LV adequacy.

As with all other lesions, TOE offers valuable information in the definition of anatomy, assessment of regurgitation jets and shunt in patients with AVSD (Fig. 25). It is particularly useful in older children and adults where the acoustic windows for TTE are limited and also in the perioperative assessment of residual lesions, stenosis or regurgitation of the AV valves as well as the estimation of the RV pressure.

Management and follow-up

Patients with AVSD will require surgery with timing depending on the degree and location of shunt. Those with large atrial and ventricular components are usually repaired between the age of 3 and 6 months. If there is shunting only at the atrial level, the natural history is similar to that observed in patients with atrial septal defects. The age of repair varies between institutions with some preferring to repair between 1 and 2 years of age (30) and other centres waiting up until 8 years (31). A significant degree of AV valve regurgitation may, however, necessitate an earlier intervention. A small number of patients with atrial shunting only are diagnosed in adolescent or adult life and are therefore repaired later.

Echocardiography (TTE, TOE, 3D) has a key role in the follow-up of these patients; residual shunts, the degree of AV valve regurgitation or narrowing and development of subaortic stenosis are the most common reasons for re-intervention.

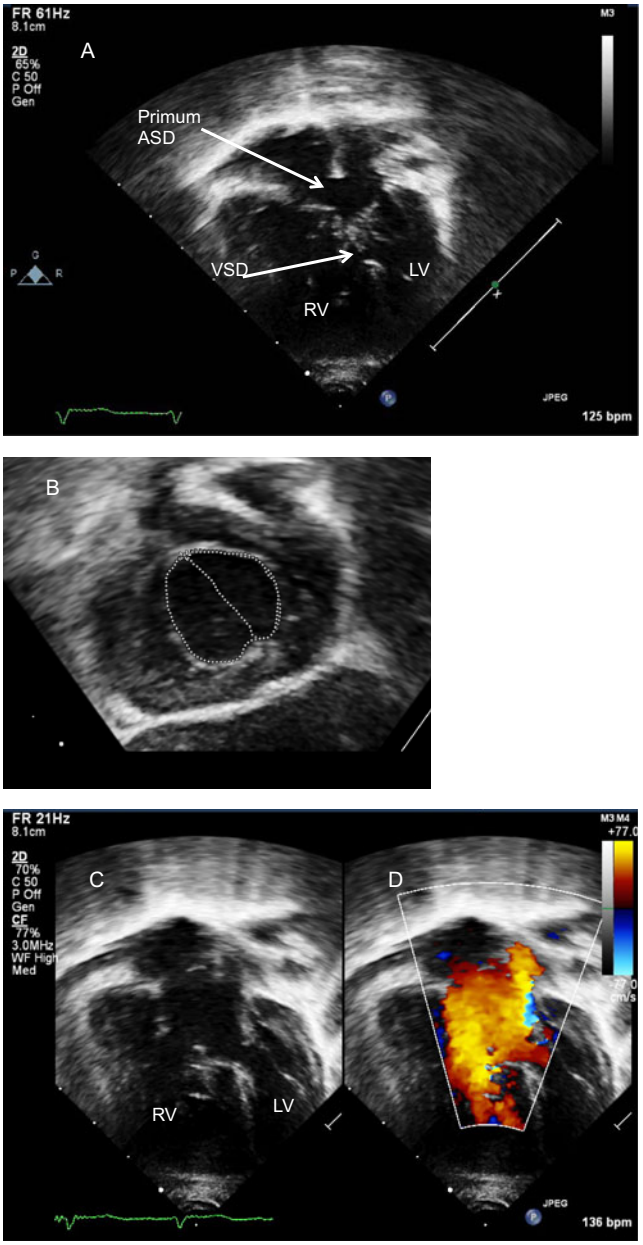

Figure 24
(A) AVSD with a degree of unbalance to the left. (B) The common valve is seen from the subcostal LAO view and the area of the left AV valve to the common AV valve is calculated (AV valve index). (C and D) The inflows are assessed on colour Doppler. Note the smaller size of the LV inflow in comparison to that on the right.

Patent arterial duct

Epidemiology and morphology

The reported incidence of a persistent duct in term neonates is only 1 in 2000 births, accounting for 5%–10% of all congenital heart disease (32). In preterm newborns the incidence is significantly higher.

www.echorespract.com
https://doi.org/10.1530/ERP-17-0062

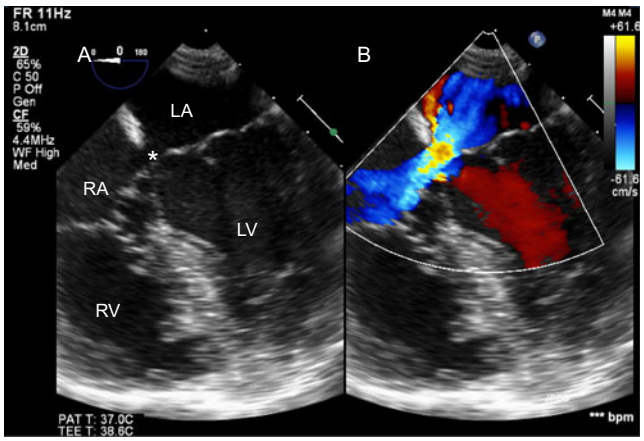

Figure 25
TOE in an adult with primum ASD (*). Colour Doppler interrogation did not reveal shunt at the ventricular level.

Echocardiographic assessment

Echocardiography is the investigation of choice in the diagnosis and assessment of the patent duct.

In neonates and infants the ductal flow can be demonstrated from several imaging views using colour Doppler but is best seen from the parasternal and suprasternal windows.

Parasternal short-axis view

The duct is seen along the left lateral border of the MPA (Fig. 26).

High left parasternal transverse view

High left parasternal transverse view shows the pulmonary artery bifurcation and the duct.

High left parasternal sagittal view ('ductal view')

This demonstrates the long axis of the duct, between the descending aorta and the LPA (Fig. 27).

Parasternal long axis view

This view allows assessment of the LV size and LA: Ao root ratio with MMode. Ratio ≥1.4 is suggestive of at least moderate shunt (33). The size of the LV is also assessed from this view and indexed to the infant's body surface area.

Suprasternal view

From the suprasternal sagittal view the arch sidedness, its branching pattern and size should be assessed and coarctation of the aorta excluded. Holodiastolic flow reversal in the descending aorta is suggestive of a

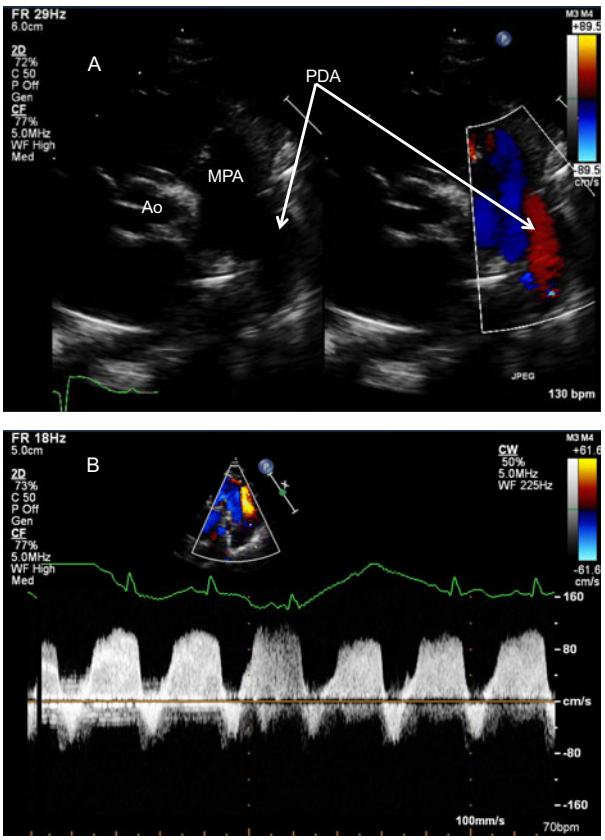

Figure 26
(A) Parasternal short-axis in a newborn with pulmonary hypertension. There is bidirectional flow across the duct, confirmed on spectral Doppler (B). Note the low velocity flow in keeping with elevated pulmonary arterial pressure.

significant shunt. The duct in a right arch can originate either from the proximal descending aorta (right duct) or the base of the left subclavian (left duct). A left duct

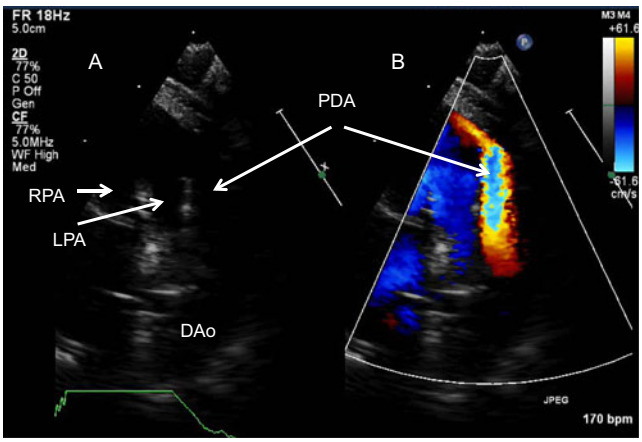

Figure 27
(A) High parasternal view on 2D shows the bifurcation of the main pulmonary artery and a large PDA with large left to right shunt (B).

in a right aortic arch with aberrant left subclavian artery confirms the diagnosis of a vascular ring.

A complete echocardiographic assessment should be performed to exclude other cardiac malformations, particularly duct dependent lesions, such as pulmonary atresia or coarctation of the aorta.

Colour Doppler is useful in the diagnosis of small ducts, not easily seen on 2D, particularly in adults with suboptimal echocardiographic windows. The flow across the duct during the cardiac cycle offers valuable information regarding the pulmonary pressure (Fig. 26).

Pitfalls in the imaging of ducts

- A large duct with right to left shunt might be difficult to identify, as the flow across it resembles the flow in the descending aorta or the LPA. Other findings suggestive of pulmonary hypertension (significant TR pressure gradient, flattening of the IVS in systole) will assist in the diagnosis. Contrast echocardiography may also be helpful; intravenous injection of agitated saline will demonstrate micro bubbles in the descending but not the ascending aorta in the presence of right to left ductal shunt.
- In some cases, a red signal along the medial border of the MPA is seen in early systole that can be confused with a duct. This is a normal flow pattern that represents helical flow in the MPA and can be differentiated by the ductal flow given its location and timing.

Management and follow-up

Haemodynamically significant ducts can be either ligated surgically or closed percutaneous with a device or coil. Post procedure the echocardiographer should look for residual shunt, evidence of pulmonary hypertension and exclude obstruction of the left pulmonary artery or arch secondary to the device. No long term follow-up is required following successful closure.

3DE in ASDs, VSDs, AVSDs

3D echocardiography is extremely useful and strongly recommended for the diagnosis, management and follow-up of patients with these lesions. The anatomy of ASDs (Fig. 12) and VSDs can be assessed with accuracy (34, 35, 36). It provides information regarding the location, shape and size of the defect (s) and the relationship with surrounding structures (Video 5). Its role is essential in planning and performing a percutaneous closure as well as in perioperative imaging. Multiplanar reformat (MPR) allows accurate measurements of the defects and facilitates the understanding of complex anatomies.

Video 5

MPR with 3D of muscular VSDs. View Video 5 at http://movie-usa.glencoesoftware.com/video/10.1530/ERP-17-0062/video-5.

3DE is outside the scope of this review. For more information please refer to the EAE/ASE recommendations for image acquisition and display using three-dimensional echocardiography (34) and the Consensus on 3DE in Congenital Heart Disease from the European Association of Cardiovascular Imaging and the ASE (35).

Conclusion

Echocardiography has a key role in the diagnosis, management and long-term follow-up of patients with left to right shunts. TTE is the investigation of choice and offers valuable information in infants and older children and can be enhanced by TOE in children and adults with suboptimal acoustic windows. 3D echocardiography is highly recommended for the examination and management of ASDs, VSDs and AVSDs. Large left to right shunts that are left untreated have a catastrophic outcome and therefore early diagnosis and careful haemodynamic assessment are paramount.

Declaration of interest

The authors declare that there is no conflict of interest that could be perceived as prejudicing the impartiality of this review.

Funding

This work did not receive any specific grant from any funding agency in the public, commercial or not-for-profit sector.

Author contribution statement

K E wrote the introduction, clinical manifestations, management and follow-up. A D wrote the morphology and echocardiographic assessment.

References

1 Hoffman JIE. The global burden of congenital heart disease. *Cardiovascular Journal of Africa* 2013 **24** 141–145. (https://doi.org/10.5830/CVJA-2013-028)

2 Levin AR, Spach MS, Boineau JP, Canent RV Jr, Capp MP & Jewett PH. Atrial pressure-flow dynamics in atrial septal defects (secundum type). *Circulation* 1968 **37** 476–488. (https://doi.org/10.1161/01.CIR.37.4.476)

3 Lopez L, Colan SD, Frommelt PC, Ensing GJ, Kendall K, Younoszai AK, Lai WW & Geva T. Recommendations for quantification methods during the performance of a pediatric echocardiogram: a report from the pediatric measurements writing group of the American Society of Echocardiography Pediatric and Congenital Heart Disease Council. *Journal of the American Society of Echocardiography* 2010 **23** 465–495. (https://doi.org/10.1016/j.echo.2010.03.019)

4 Rudski LG, Lai WW, Afilalo J, Hua L, Handschumacher MD, Chandrasekaran K, Solomon SD, Louie EK & Schiller NB. Guidelines for the echocardiographic assessment of the right heart in adults: a report from the American Society of Echocardiography. *Journal of the American Society of Echocardiography* 2010 **23** 685–713. (https://doi.org/10.1016/j.echo.2010.05.010)

5 Helbing WA, Bosch HG, Maliepaard C, Rebergen SA, van der Geest RJ, Hansen B, Ottenkamp J, Reiber JH & de Roos A. Comparison of echocardiographic methods with magnetic resonance imaging for assessment of right ventricular function in children. *American Journal of Cardiology* 1995 **76** 589–594. (https://doi.org/10.1016/S0002-9149(99)80161-1)

6 Alghamdi MH, Grosse-Wortmann L, Ahmad N, Mertens L & Friedberg MK. Can simple echocardiographic measures reduce the number of cardiac magnetic resonance imaging studies to diagnose right ventricular enlargement in congenital heart disease? *Journal of the American Society of Echocardiography* 2012 **25** 383–384. (https://doi.org/10.1016/j.echo.2011.12.022)

7 Gopal AS, Chukwu EO, Iwuchukwu CJ, Katz AS, Toole RS, Schapiro W & Reichek N. Normal values of right ventricular size and function by real-time 3-dimensional echocardiography: comparison with cardiac magnetic resonance imaging. *Journal of the American Society of Echocardiography* 2007 **20** 445–455. (https://doi.org/10.1016/j.echo.2006.10.027)

8 Lu X, Nadvoretskiy V, Bu L, Stolpen A, Ayres N, Pignatelli RH, Kovalchin JP, Grenier M, Klas B & Ge S. Accuracy and reproducibility of real-time three-dimensional echocardiography for assessment of right ventricular volumes and ejection fraction in children. *Journal of the American Society of Echocardiography* 2008 **21** 84–89. (https://doi.org/10.1016/j.echo.2007.05.009)

9 Jenkins C, Chan J, Bricknell K, Strudwick M & Marwick TH. Reproducibility of right ventricular volumes and ejection fraction using real-time three-dimensional volumes using real-time three-dimensional echocardiography: comparison with cardiac MRI. *Chest* 2007 **131** 1844–1851. (https://doi.org/10.1378/chest.06-2143)

10 Rufino Nascimento IG, Dehant P, Jimenez M, Dequeker JL, Castela E & Choussat A. Calculation of the pulmonary to systemic flow ratio using echo-Doppler in septal defects-correlation with oximetry. *Revista Portuguesa de Cardiologia* 1989 **8** 35–40.

11 Schubert S, Peters B, Abdul-Khaliq H, Nagdyman N, Lange PE & Ewert P. Left ventricular conditioning in the elderly patient to prevent congestive heart failure after transcatheter closure of atrial septal defect. *Catheterization and Cardiovascular Interventions* 2005 **64** 333–337. (https://doi.org/10.1002/ccd.20292)

12 Anderson RH. Interatrial communications. In *Paediatric Cardiology*, 3rd edn., ch 25, p 529. Eds RH Anderson, EJ Baker, DJ Penny, AN Redington, ML Rigby & G Wernovsky. Philadelphia, PA, USA: Churchill Livingstone, 2010.

13 McCarthy K, Ho S & Anderson R. Defining the morphology phenotypes of atrial septal defects and interatrial communications. *Images in Paediatric Cardiology* 2003 **5** 1–24.

14 Hahn RT, Abraham T, Adams MS, Bruce CJ, Glas KE, Lang RM, Reeves ST, Shanewise JS, Siu SC, Stewart W, *et al*. Guidelines for performing a comprehensive transesophageal echocardiographic examination: recommendations from the American Society of Echocardiography and the Society of Cardiovascular Anesthesiologists. *Journal of the American Society of Echocardiography* 2013 **26** 921–964. (https://doi.org/10.1016/j.echo.2013.07.009)

15 Silvestry F, Cohen M, Armsby LB, Burkule NJ, Fleishman CE, Hijazi ZM, Lang RM, Rome JJ & Wang Y. Guidelines for the echocardiographic assessment of atrial septal defect and patent foramen ovale: from the American Society of Echocardiography and Society for Cardiac Angiography and Interventions. *Journal of the American Society of Echocardiography* 2015 **28** 910–958. (https://doi.org/10.1016/j.echo.2015.05.015)

16 Abaci A, Unlu S, Alsancak Y, Kaya U & Sezenoz B. Short and long term complications of device closure of atrial septal defect and patent foramen ovale: meta analysis of 28,142 patients from 203 studies. *Catheterization and Cardiovascular Interventions* 2013 **82** 1123–1138. (https://doi.org/10.1002/ccd.24875)

17 Young D. Later results of closure of secundum atrial septal defect in children. *American Journal of Cardiology* 1973 **31** 14–22. (https://doi.org/10.1016/0002-9149(73)90804-7)

18 Bricker JT, Gillette PC, Cooley DA & McNamara DG. Dysrhythmias after repair of atrial septal defect. *Texas Heart Institute Journal* 1986 **13** 203–208.

19 Lewis DA, Loffredo CA, Correa-Villaseñor A, Wilson PD & Martin GR. Descriptive epidemiology of membranous and muscular ventricular septal defects in the Baltimore-Washington Infant Study. *Cardiology in the Young* 1996 **6** 281–290.

20 Anderson RH. Ventricular septal defects. In *Paediatric Cardiology*, 3rd edn., ch 28, pp 594–605. Eds RH Anderson, EJ Baker, DJ Penny, AN Redington, ML Rigby & G Wernovsky. Philadelphia, PA, USA: Churchill Livingstone, 2010.

21 McCarthy KP, Ho SY & Anderson RH. Categorisation of ventricular septal defects: review of the perimembranous morphology. *Images in Paediatric Cardiology* 2000 **2** 24–40.

22 Jacobs JP, Burke RP, Quintessenza JA & Mavroudis C. Congenital heart surgery nomenclature and database project: ventricular septal defect. *Annals of Thoracic Surgery* 2000 **69** S25–S35. (https://doi.org/10.1016/S0003-4975(99)01270-9)

23 Forbus GA & Shirali GS. Anomalies of the ventricular septum. In *Echocardiography in Paediatric and Congenital Heart Disease from Fetus to Adult*, 1st ed., ch 12, p 180. Eds WW Lai, LL Mertens, MS Cohen & T Geva. Hoboken, NJ, USA: John Wiley & Sons Ltd, 2009.

24 Hoffman JI & Kaplan S. The incidence of congenital heart disease. *JACC: Journal of the American College of Cardiology* 2002 **39** 1890–1900. (https://doi.org/10.1016/S0735-1097(02)01886-7)

25 Bergström S, Carr H, Petersson G, Stephansson O, Edstedt Bonamy AK, Dahlström A, Pegelow Halvorsen C & Johansson S. Trends in congenital heart defects in infants with Down syndrome. *Pediatrics* 2016 **138** e20160123.

26 Ebels T, Elzenga N & Anderson RH. Atrioventricular septal defects. In *Paediatric Cardiology*, 3rd ed., ch 27, pp 560–564. Eds RH Anderson, EJ Baker, DJ Penny, AN Redington, ML Rigby & G Wernovsky. Philadelphia, PA, USA: Churchill Livingstone, 2010.

27 Draulans-Noë HA, Wenink AC & Quaegebeur J. Single papillary muscle ("parachute valve") and double-orifice ventricle in atrioventricular septal defects convergence of chordal attachments: surgical anatomy and results of surgery. *Pediatric Cardiology* 1990 **11** 29–35.

28 Jegatheeswaran A, Pizarro C, Caldarone CA, Cohen MS, Baffa JM, Gremmels DB, Mertens L, Morrell VO, Williams WG, Blackstone EH, *et al*. Echocardiographic definition and surgical decision-making in unbalanced atrioventricular septal defect. *Circulation* 2010 **122** S209–S215. (https://doi.org/10.1161/CIRCULATIONAHA.109.925636)

29 Cohen MS, Jegatheeswaran A, Baffa JM, Gremmels DB, Overman DM, Caldarone CA, McCrindle BW & Mertens L. Echocardiographic features defining right dominant unbalanced atrioventricular septal defect. A multi-institutional Congenital Heart Surgeons' Society Study. *Circulation: Cardiovascular Imaging* 2013 **6** 508–513.

30 Devlin PJ, Backer CL, Eltayeb O, Mongé MC, Hauck AL & Costello JM. Repair of partial atrioventricular septal defect: age and outcomes. *Annals of Thoracic Surgery* 2016 **102** 170–177. (https://doi.org/10.1016/j.athoracsur.2016.01.085)

31 Bowman JL, Dearani JA, Burkhart HM, Goodloe AH, Phillips SD, Weaver AL, Eidem BW & Cetta F. Should repair of partial atrioventricular septal defect be delayed until later in childhood? *American Journal of Cardiology* 2014 **114** 463–467. (https://doi.org/10.1016/j.amjcard.2014.05.020)
32 Schneider DJ & Moore JW. Patent ductus arteriosus. *Circulation* 2006 **114** 1873–1882. (https://doi.org/10.1161/CIRCULATIONAHA.105.592063)
33 Johnson GL, Breart GL, Gewitz MH, Brenner JI, Lang P, Dooley KJ & Curtis Ellison R. Echocardiographic characteristics of premature infants with patent ductus arteriosus. *Pediatrics* 1983 **72** 864–871.
34 Lang RM, Badano LP, Tsang W, Adams DH, Agricola E, Buck T, Faletra FF, Franke A, Hung J, de Isla LP, *et al*. EAE/ASE recommendations for image acquisition and display using three-dimensional echocardiography. *Journal of the American Society of Echocardiography* 2012 **25** 3–46. (https://doi.org/10.1016/j.echo.2011.11.010)
35 Simpson J, Lopez L, Acar P, Friedberg MK, Khoo NS, Ko HH, Marek J, Marx G, McGhie JS, Meijboom F, *et al*. Three-dimensional echocardiography in congenital heart disease: an expert consensus document from the European Association of Cardiovascular Imaging and the American Society of Echocardiography. *Journal of the American Society of Echocardiography* 2017 **30** 1–27. (https://doi.org/10.1016/j.echo.2016.08.022)
36 Cossor W, Cui VW & Roberson DA. Three-dimensional echocardiography en face views of ventricular septal defects: feasibility, accuracy, imaging, protocols and reference image collection. *Journal of the Americal Society of Echocardiography* 2015 **28** 1020–1029. (https://doi.org/10.1016/j.echo.2015.05.014)

Received in final form 28 January 2018
Accepted 5 February 2018
Accepted Preprint published online 5 February 2018